

The effects of cooling conditions on surface integrity in machining of Ti6Al4V alloy

*Original*

The effects of cooling conditions on surface integrity in machining of Ti6Al4V alloy / G., Rotella; O. W., Dillon; D., Umbrello; Settineri, Luca; I. S., Jawahir. - In: INTERNATIONAL JOURNAL, ADVANCED MANUFACTURING TECHNOLOGY. - ISSN 0268-3768. - STAMPA. - 71:(2013), pp. 47-55. [10.1007/s00170-013-5477-9]

*Availability:*

This version is available at: 11583/2543090 since:

*Publisher:*

Springer

*Published*

DOI:10.1007/s00170-013-5477-9

*Terms of use:*

This article is made available under terms and conditions as specified in the corresponding bibliographic description in the repository

*Publisher copyright*

(Article begins on next page)

1  
2  
3  
4  
5  
6  
7  
8  
9  
10  
11  
12  
13  
14  
15  
16  
17  
18  
19  
20  
21  
22  
23  
24  
25  
26  
27  
28  
29  
30  
31  
32  
33  
34  
35  
36  
37  
38  
39  
40  
41  
42  
43  
44  
45  
46  
47  
48  
49  
50  
51  
52  
53  
54  
55  
56  
57  
58  
59  
60  
61  
62  
63  
64  
65

# The effects of Cooling Conditions on Surface Integrity in Machining of *Ti6Al4V* Alloy

G. Rotella<sup>1,2</sup>, O.W. Dillon, Jr.<sup>2</sup>, D. Umbrello<sup>1,2\*</sup>, L. Settineri<sup>3</sup>, I.S. Jawahir<sup>2</sup>

<sup>1</sup>*Department of Mechanical, Energy and Management Engineering, University of Calabria,  
Rende (CS) 87036, Italy*

<sup>2</sup>*Institute for Sustainable Manufacturing (ISM), University of Kentucky, Lexington (KY)  
40506, USA*

<sup>3</sup>*Department of Management and Production Engineering, Politecnico di Torino, Torino  
(TO) 10129, Italy*

## **Abstract**

This paper presents results from a comparative study of machining of *Ti6Al4V* alloy under dry, MQL and cryogenic cooling conditions using coated tools at varying cutting speeds and feed rates. The influence of the cooling conditions on surface integrity and the product performance was studied in terms of surface roughness, metallurgical conditions, including microstructure, hardness, grain refinement and phase transformation of the machined product. Results show that cooling conditions affect surface integrity of the product signifying the benefits of cryogenic cooling in improving the overall product performance.

**Keywords:** *Machining; Surface Integrity; Cryogenic Cooling; Ti6Al4V.*

---

\* Corresponding author: d.umbrello@unica.it; Tel.: +39-0984 494820. Fax: +39-0984 494673.

## 1. INTRODUCTION

1  
2  
3 Global competitive market in manufacturing demands high quality products at reduced costs  
4  
5 and improved productivity rates. Advanced technological solutions are urged for globally-  
6  
7 competitive sustainable manufacturing [1]. The aircraft industry is one of the most relevant  
8  
9 **example** where all finished products must be produced with consistently high quality, to  
10  
11 ensure high safety standards for performance over the lifetime. In the manufacture of  
12  
13 aerospace components, surface integrity plays a key role due to its strong correlation with the  
14  
15 functional performance and service-life of such engineered components. Numerous aircraft  
16  
17 components are produced exclusively by a range of machining operations. Their use and  
18  
19 functional performance heavily depend on being able to design and manufacture these  
20  
21 components with high degree of reliability and predictability of their functionality and safety.  
22  
23 Surface characteristics of machined products such as microstructure, surface roughness,  
24  
25 hardness and residual stresses are among the most significant characteristics determining the  
26  
27 reliability and the functional performance of a product [2]. A long-lasting product satisfying  
28  
29 high quality standards helps to save energy and costs during its functional performance, and  
30  
31 therefore can be considered more sustainable. A sustainable product would not only require  
32  
33 less-frequent replacement with upgradability and maintainability, but also must demonstrate  
34  
35 high reliability and improved safety during its service life [3]. Metalworking fluids (MWFs)  
36  
37 have generally been considered highly-effective, and as integral part of manufacturing  
38  
39 processes for decades, despite conflicting studies showing the actual effectiveness of their use  
40  
41 in several operations in terms of unfavorable product and process performance results. Over  
42  
43 the years, the MWFs have also changed dramatically, due to high demands to provide better  
44  
45 performance, and facilitate improved health and safety conditions. In metal machining, the  
46  
47 use of cutting fluids is regarded as an area for potential improvement because of the serious  
48  
49 health and environmental threat associated with their use, disposal and related high costs.  
50  
51  
52  
53  
54  
55  
56  
57  
58  
59  
60  
61  
62  
63  
64  
65

1 Thus, various researchers have examined the benefits, drawbacks and conditions necessary for  
2 machining a range of materials with dedicated cooling methods such as flood-cooling, dry and  
3  
4 MQL machining [4-8].  
5  
6

7 At the onset, it appears that the most-promising idea would be to use a more sustainable and  
8  
9 cost-effective process by eliminating the traditional MWFs, since they are not embodied in  
10  
11 final products. However, since MWFs are often required to produce high performance  
12  
13 products, their elimination is not always possible, especially when difficult-to-cut materials  
14  
15 are machined [4].  
16  
17

18  
19 Several conscious cooling approaches [4, 9, 10] have been widely investigated in the recent  
20  
21 time, especially for difficult-to-cut materials. In particular, liquid nitrogen (LN<sub>2</sub>) has been  
22  
23 applied as a cryogenic coolant and, consequently, it has been widely investigated, especially  
24  
25 for machining *Ti6Al4V* titanium alloy [11-15]. Most of the research demonstrated  
26  
27 improvements in various aspects of *Ti6Al4V* machinability, either by cryogenically freezing  
28  
29 the workpiece or by spraying LN<sub>2</sub> to the cutting zone. The main functions of cryogenic  
30  
31 cooling in metal cutting were defined by Hong and Zhao [11] as effectively removing heat  
32  
33 from the cutting zone. Hence, it has the potential to decrease the cutting temperatures [16],  
34  
35 modify the frictional characteristics at the tool/chip interfaces[17], change the properties of  
36  
37 the workpiece and the tool material [18].  
38  
39  
40  
41  
42

43 Other research showed the effects of different cooling strategies, including cryogenic cooling,  
44  
45 on surface and sub-surface hardness, founding that it generally increases when a drastic  
46  
47 cooling is applied [14, 19]. Particularly, specimens of *Ti6Al4V* alloys machined under  
48  
49 cryogenic cooling showed rapid increase in their strength and hardness, while their toughness  
50  
51 and ductility showed little variation as the temperature decreases [15]. Therefore,  
52  
53 simultaneously cooling the workpiece to enhance the chemical stability of the workpiece, and  
54  
55 cooling the cutting tool to enhance the hardness and chemical stability of the tool, were  
56  
57 recommended as an effective cryogenic strategy for titanium alloy [15].  
58  
59  
60  
61  
62  
63  
64  
65

1 Furthermore, it was also stated that liquid nitrogen should have some sort of positive  
2 boundary lubrication effect [17]. Strong adhesion between tool rake and chip face occurs in  
3  
4 dry cutting conditions and lower temperatures could make the material harder and less sticky  
5  
6 by reducing adhesion between the interacting surfaces resulting in a low friction [17]. As a  
7  
8 consequence, the reduced friction coefficient at the tool-chip interface generates lower cutting  
9  
10 forces than those observed in dry machining.  
11  
12

13 Finally, it has been also reported that cryogenic process successfully generates thicker surface  
14  
15 layers consisting of ultrafine/nano-grain structures on different materials such as steels, *Ni* and  
16  
17 *Mg* alloys [20-22]. Along with the benefits on grain refinement, cryogenic under severe  
18  
19 plastic deformation (*SPD*) is also expected to introduce compressive residual stresses on the  
20  
21 surface and sub-surface layers [23].  
22  
23  
24

25 In summary, the cryogenic processing-induced surface integrity modifications can be  
26  
27 beneficial for a series of processes and products performance. However, very few studies have  
28  
29 been devoted to quantify these simultaneous changes in surface integrity during cryogenic  
30  
31 processing [23-25], whereas no complete investigation on surface integrity are done when *Ti*  
32  
33 alloys are investigated, but only studies on cryogenic cooling influence on surface roughness  
34  
35 are reported [26-27]. Therefore, the main objective of this paper is to investigate and establish  
36  
37 the effects of different cooling/lubricating conditions on surface integrity (surface roughness,  
38  
39 hardness modification, phase changes, grain size, etc.) in machining of *Ti6Al4V* alloy at  
40  
41 varying cutting speeds and feed rates, to enable optimized product performance.  
42  
43  
44  
45  
46  
47  
48  
49  
50

## 51 **2. EXPERIMENTAL PROCEDURE**

52 The orthogonal cutting operation was conducted on a Mazak QuickTurn10 CNC turning  
53  
54 center, and it involved radially cutting of the *Ti6Al4V* (354 HV) disks at feed rates of 0.1 and  
55  
56 0.05 mm/rev at three cutting speeds (Table 1). The cutting tests were designed to avoid  
57  
58  
59  
60  
61  
62  
63  
64  
65

1 undesired effects on the machined surface related to transient conditions. At the prescribed  
2 end-of-cut, the cutting tool was instantaneously retracted at maximum feed to avoid the  
3 rubbing of the tool against the machined workpiece surface. The utilized cutting tool inserts  
4 are coated carbides, Kennametal® KCU10 grade, with an advanced PVD *TiAlN* coating, and  
5 are of triangular shape - TNGG432FS series, mounted on a MTCNN-124 tool holder  
6  
7 (providing rake and clearance angles of 7° and 11°, respectively). The measured initial cutting  
8 edge radius, prior to machining was consistent, and was in the range of 8 – 10 microns in all  
9 tested tool inserts.  
10

11 The effect of variations in cutting edge radius during each test was avoided by allowing fresh  
12 cutting edge for each test of short duration. The MQL tests were performed applying  
13 vegetable oil emulsion through an external nozzle to the cutting zone properly selecting a  
14 flow rate of 60 ml/hr [28]. (with a pressure of 4 bar), while the cryogenic coolant (LN<sub>2</sub>) was  
15 applied through a 2 mm nozzle (with a pressure of 12 bar) to the cutting region, thus creating  
16 a surface temperature of -185 °C. After machining, all samples were metallographically-  
17 processed: sectioned, mounted on a resin holder, and then polished and etched. The etchant  
18 employed is the Kroll's reagent that is recommended for etching nonferrous materials and  
19 recommended for *Ti* alloys. The composition of the reagent is 92 ml of distilled water, 6 ml of  
20 Nitric acid and 2 ml of Hydrochloric acid. A fresh etchant was used for each sample and the  
21 immersion time was around 20 second for each sample. The microstructural changes have  
22 been analyzed using a Scanning Electronic Microscopy (SEM). The surface and subsurface  
23 hardness values were also measured on a micro hardness indenter Future Tech F-7. The  
24 surface roughness was measured and analyzed using a Zygo7300® optical white light  
25 interferometry-based surface profilometer. Additionally, XRD patterns between 30 and 75  
26 deg 2θ of the processed surfaces were also acquired for investigating the phase transformation  
27 taking place on the machined surface. The X-ray diffractometer used *Cu-Kα* radiation  
28  
29  
30  
31  
32  
33  
34  
35  
36  
37  
38  
39  
40  
41  
42  
43  
44  
45  
46  
47  
48  
49  
50  
51  
52  
53  
54  
55  
56  
57  
58  
59  
60  
61  
62  
63  
64  
65

1  
2  
3  
4  
5  
6  
7  
8  
9  
10  
11  
12  
13  
14  
15  
16  
17  
18  
19  
20  
21  
22  
23  
24  
25  
26  
27  
28  
29  
30  
31  
32  
33  
34  
35  
36  
37  
38  
39  
40  
41  
42  
43  
44  
45  
46  
47  
48  
49  
50  
51  
52  
53  
54  
55  
56  
57  
58  
59  
60  
61  
62  
63  
64  
65

( $\lambda=1.54184\text{\AA}$ ,  $K\alpha_1/K\alpha_2=0.5$ ) from a source operated at 40 kV, and 40 mA. Samples were accordingly positioned at the center of plate into the X-ray goniometric in order to guarantee a correct beam radiation. The scan increment was 0.05 degree.

### 3. EXPERIMENTAL RESULTS AND DISCUSSION

#### 3.1 Surface roughness

The surface roughness of each test was measured five times at different locations along the surface. The observed trend for the mean surface roughness  $R_a$  is reported in Figure 2 (a) for a feed rate of 0.05 mm/rev, while in Figure 2 (b) the results for a feed rate of 0.1 mm/rev are reported. A decreasing trend for the mean surface roughness  $R_a$  is seen, when the cutting speed increases. The feed rate seems to have a very minor influence on the roughness trend.

The  $R_a$  measurements obtained in machining with cryogenic coolant were found to be largely and consistently superior to those obtained in dry and MQL machining, and at higher cutting speed, MQL produced comparable results. The overall surface roughness for all three cooling conditions is always below 0.3  $\mu\text{m}$ , which is a very good finish surface quality. It has been shown that, a smooth surface with better surface roughness would prevent the initiation of cracks under cyclic loads [29].

#### 3.2. Surface and sub-surface hardness

Figure 3 (a) shows the surface hardness of the samples machined at 0.05 mm/rev feed rate, while the results related to the higher feed rate are reported in Figure 3 (b). The results clearly demonstrate that cryogenic cutting condition allows the material to reach a higher surface hardness in all the test conditions.

Figure 4 shows the hardness variation of machined samples at 0.1 mm/rev from the surface to the bulk material. A deeper hardness alteration is verified in all cryogenically-machined

1 samples. MQL performs better than dry machining by exhibiting a higher surface hardness,  
2 and maintaining it up to a greater depth.  
3

4 Dry cutting with its higher temperatures does not allow an increase in the surface and  
5 subsurface hardness, and cryogenic machining with its lower temperatures promotes the  
6 hardness increase during the cutting process. In fact, a combination of reduced thermal  
7 softening effect and greater grain refinement results in a higher surface hardness in the  
8 machined samples.  
9

10 On the other hand, dry machining, due to the lack of coolant, tends to create softer and  
11 rougher surfaces. Hardness induced by the use of MQL during machining lies between the dry  
12 and the cryogenic cooling since the mix of lubricant and pressurized air slightly reduces the  
13 temperature during cutting. However, the MQL cooling effect, including the rate and  
14 intensity, is not comparable with that developed during cryogenic machining due to its  
15 significantly reduced thermal gradient and capacity.  
16  
17  
18  
19  
20  
21  
22  
23  
24  
25  
26  
27  
28  
29  
30

### 31 **3.3. Microstructure**

32 The grain size and shape, and the grain boundary arrangements in *Ti* alloys have a significant  
33 influence on the induced mechanical properties of the machined component. The ability to  
34 manipulate the phase/grains present, by alloying, is responsible for achieving desirable  
35 properties in *Ti* and its alloys [30]. It is generally known that the microstructure influences the  
36 behavior of the *Ti* alloys, and a refined grain structure is more desirable from the point of  
37 view of tensile yield stress in metallic materials. In contrast, the ultimate tensile stress of *Ti*  
38 alloys is not significantly influenced by grain size, but its ductility, as represented by  
39 elongation or reduction in area, and it generally is improved with smaller grain size [30].  
40 Also, fatigue life can strongly depend on this parameter [31-33]. Thus, the grain size was  
41  
42  
43  
44  
45  
46  
47  
48  
49  
50  
51  
52  
53  
54  
55  
56  
57  
58  
59  
60  
61  
62  
63  
64  
65



1 measured on each machined surface as well as on the as received material using both an  
2 optical and SEM microscope.  
3

4 The microstructure of the as-received *Ti6Al4V* used in this study is shown in Fig. 5; the dark  
5 region is the  $\alpha$  phase and the light region is the  $\beta$  phase. The  $\alpha$  grains were measured to be  
6 around 20  $\mu\text{m}$ .  
7  
8  
9

10 Generally, higher  $\alpha$  content results in higher creep resistance and high-temperature strength,  
11 while higher  $\beta$  content leads to higher density and room temperature strength [30]. However,  
12 the combination of softer  $\alpha$  grains and harder  $\beta$  phase is usually preferred for achieving good  
13 performance in an alloy for the strength and the fatigue life [30].  
14  
15  
16  
17  
18  
19  
20  
21

22 Figures 6 shows the SEM microstructures of the machined samples at  $v_c = 150$  m/min, and  $f$   
23 = 0.05 mm/rev. These results show that both the bulk material and the machined surface  
24 present an equiaxed microstructure of primary  $\alpha$  grains and intergranular beta ( $\beta$ ) grains.  
25  
26  
27  
28

29 Also, the structure near the machined surface presents a more dense the  $\beta$  phase leading to  
30 higher room temperature strength [30].  
31  
32  
33  
34

35 All the examined samples present a refinement of the mean grain diameter from the bulk to  
36 the surface although the grain refinement is more evident for MQL and cryogenic conditions,  
37 where the microstructures are more dense and present a deeper SPD layer. Figure 7 highlights  
38 how the lubricant/coolant and the processing parameter affect the microstructure of the  
39 machined samples showing the grain refinement evolution from the less influencing condition  
40 (70 m/min, 0.05 mm/rev, dry cutting) to the most effecting condition (150 m/min, 0.10  
41 mm/rev, cutting under cryogenic cooling).  
42  
43  
44  
45  
46  
47  
48  
49  
50  
51

52 It is worth to point out that the process parameters influence a lot the microstructural changes  
53 under dry conditions while the cooling effect of cryogenic prevails on the microstructural  
54 behavior. This trend is better shown in Figure 8 where the grain size on the machined surface  
55 for all the experimental tests are reported. Obtaining smaller grains when using cryogenic  
56  
57  
58  
59  
60  
61  
62  
63  
64  
65

1 cooling conditions is related to the fact that this cooling process prevents grain growth after  
2 the dynamic recrystallization (DRX), which in turn is the result of the severe plastic  
3 deformation process [34]. These results also confirm the potential of the use of cryogenic  
4 cooling to generate a stronger machined product, with a harder surface, and less prone to  
5 crack initiation [31, 32, 34].  
6  
7  
8  
9  
10

### 11 **3.4. Phase changes – XRD analysis**

12 Phase change is a microstructural feature that cannot be optically detected, but it strongly  
13 influences the material properties. For example, transformed  $\beta$  phase products in *Ti* alloys can  
14 affect tensile strengths, ductility, toughness, and cyclic properties [30]. Processing of *Ti6Al4V*  
15 alloy can lead to formation of two secondary phases: *Ti3Al* and  $\omega$  on the surface. *Ti3Al* is  
16 detrimental to the resistance to stress corrosion of the material; while the  $\omega$  phase is  
17 undesirable due to its brittleness [30]. First of all, it is important to underline that X-ray  
18 diffraction of all the investigated samples does not show any peak corresponding to *Ti3Al* or  
19  $\omega$  phase formation.  
20  
21  
22  
23  
24  
25  
26  
27  
28  
29  
30  
31  
32  
33  
34  
35

36 Figure 9 shows the XRD patterns for some of the investigated cutting conditions in which the  
37  $\alpha$  and  $\beta$  phases were identified according to Bragg's law and data reported in the materials  
38 Handbook [35]. The results generally show that the  $\beta$  transus temperature was never reached  
39 during the process since the  $\alpha$  phase does not significantly decrease in peak intensity [36].  
40 However, the  $\beta$  peak changes with the process conditions and the lubricant/coolant used. In  
41 particular, it increases under dry condition and slightly increases with the cutting speed. In  
42 contrast, the feed rate does not significantly affect the  $\beta$  peak.  
43  
44  
45  
46  
47  
48  
49  
50  
51  
52  
53

54 Another cardinal aspect to be highlighted from the XRD analysis is related to the relative  
55 intensity and the width, which are influenced from cutting process and cooling condition.  
56 According to Herbert et al. [37] different intensity represents different grain size. As it is  
57  
58  
59  
60  
61  
62  
63  
64  
65

1 clearly seen in Fig. 7, primary  $\alpha$  grains refinements are observed when higher cutting speeds  
2 and cryogenic cooling are utilized. The XRD profiles, in term of intensity and width of the  
3  
4  
5  $\alpha$  peak (Figure 9), are in accordance with the grain size trends reported in Figure 9.

6  
7 Also, the ratio of the two phases influences the behavior of *Ti* alloys, and therefore it is crucial  
8  
9 to identify these differences in the processed material [38]. In fact, the  $\alpha$  phase partially  
10  
11 transforms to the  $\beta$  phase at temperatures above  $\alpha / (\alpha+\beta)$  transus [38]. Thus, the volume  
12  
13 fraction of  $\alpha$  and  $\beta$  phases was calculated from the XRD results as follows [39]:  
14  
15

$$\frac{I_{\beta}}{I_{\alpha}} = A \frac{f_{\beta}}{f_{\alpha}} \quad (1)$$

16  
17  
18  
19  
20  
21  
22  
23  
24  
25  
26 where  $I$  is the peak intensity of the interested phase and  $f$  its volume fraction, and  $A$  is the ratio  
27  
28 between the relative integrated intensities of both phases [39]. According to each XRD  
29  
30 spectrum, the  $\beta$  percentage increases from the 11% in the unprocessed material to the 30% in  
31  
32 the machined surface in dry machining at 150 m/min and 0.1 mm/rev. The peak ratios show a  
33  
34 similar trend between cryogenic and MQL coolants, which exhibit a slightly lower  $\beta$   
35  
36 percentage than dry machining (about 22% for cryogenic and 25% for MQL). In contrast, the  
37  
38 feed rate slightly affects the volume fraction variation, while the  $\beta$  percentage decreases when  
39  
40 increasing the cutting speed. The  $\beta$  phase is not materially so different from the  $\alpha+\beta$  phase  
41  
42 even if, an increase of the  $\beta$  phase on the surface can increase the efficiency of the material  
43  
44 since the formation of a little  $\beta$  permits the alloy to be strengthened [30]. However, a  
45  
46 reduction of grain size is more effective than a decrease of primary  $\alpha$  volume fraction for  
47  
48 improving the fatigue life in, both the low cycle fatigue (LCF), and high cycle fatigue (HCF)  
49  
50 ranges [30]. The effectiveness of strengthening in *Ti* alloys appears to be more influenced by  
51  
52 the number and fineness of phase boundaries and the grain size [30].  
53  
54  
55  
56  
57  
58  
59  
60  
61  
62  
63  
64  
65

#### 4. CONCLUSIONS

Experimental observations reported in this paper show the capability of cryogenic cooling to improve the product surface integrity in machining of *Ti6Al4V* alloys. In particular, the surface roughness strongly benefits from the use of cryogenic cooling as well as the hardness at the surface and sub-surface level. Furthermore, the surface microstructural changes highlight how cryogenic coolant improves the DRX mechanism containing the regrowth phase. Thus, cryogenically-machined samples generally show a superior surface finishing (combination of mean surface roughness, microhardness and grain size), which is partially reached by MQL machined specimens only under certain conditions. In contrast, dry machining permits to achieve a higher  $\beta$  volume fraction, which is beneficial for increased material strength at room temperature.

From a sustainability perspective, cryogenic machining is more environmentally-friendly when compared with the traditional flood cooling methods and MQL machining. It also contributes to make products having better surface integrity and quality by generating smaller grains.

Overall, this study demonstrates that the different cooling/lubrication methods affect the surface characteristics of *Ti6Al4V* alloy. In particular, cryogenic cooling can significantly improve the product surface characteristics having a great impact on its quality and potentially improve its reliability.

#### ACKNOWLEDGMENTS

The authors gratefully acknowledge the help provided by Tao Lu and Charles Arvin during the experimental work conducted at the Institute for Sustainable Manufacturing, University of Kentucky and Mr. J. Backus from Kentucky Geological Survey for his help with the XRD

1  
2 measurements. The authors should also like to acknowledge Mr. Steve Chen of Kennametal  
3 Tools for the donation of cutting tools.  
4  
5  
6

## 7 **REFERENCES**

- 8  
9  
10 [1] Jovane F, Yoshikawa H, Alting L, Boer CR, Westkamper E, Williams D, Tseng M,  
11 Seliger G, Paci AM (2008) The incoming global technological and industrial revolution  
12 towards competitive sustainable manufacturing. *CIRP Annals – Manuf Technol*  
13 57(2):641–659.  
14  
15 [2] Jawahir IS, Brinksmeier E, M’Saoubi R, Aspinwall DK, Outeiro JC, Meyer D,  
16 Umbrello D, Jayal AD (2011) Surface integrity in material removal processes: Recent  
17 advances. *CIRP Annals – Manuf Technol* 60(2):603–626.  
18  
19 [3] Jayal AD, Badurdeen F, Dillon Jr. OW, Jawahir IS (2010) Sustainable manufacturing:  
20 Modeling and optimization challenges at the product, process and system levels. *CIRP J*  
21 *Manuf Sci Technol* 2(3):144–152.  
22  
23 [4] Shokrani A, Dhokia V, Newman ST (2012) Environmentally conscious machining of  
24 difficult-to-machine materials with regard to cutting fluids. *Int J Mach Tools Manuf*  
25 57:83–101.  
26  
27 [5] Klocke F, Eisenblatter G (1997) Dry Cutting. *CIRP Annals – Manuf Technol*  
28 46(2):519–526.  
29  
30 [6] Jayal AJ, Balaji AK (2009) Effects of cutting fluid application on tool wear in  
31 machining: Interactions with tool-coatings and tool surface features. *Wear* 267(9):1723–  
32 1730.  
33  
34 [7] Weinert K, Inasaki I, Sutherland JW, Wakabayashi T (2004) Dry Machining and  
35 Minimum Quantity Lubrication. *CIRP Annals – Manuf Technol* 53(2):511–537.  
36  
37  
38  
39  
40  
41  
42  
43  
44  
45  
46  
47  
48  
49  
50  
51  
52  
53  
54  
55  
56  
57  
58  
59  
60  
61  
62  
63  
64  
65

- 1  
2  
3  
4  
5  
6  
7  
8  
9  
10  
11  
12  
13  
14  
15  
16  
17  
18  
19  
20  
21  
22  
23  
24  
25  
26  
27  
28  
29  
30  
31  
32  
33  
34  
35  
36  
37  
38  
39  
40  
41  
42  
43  
44  
45  
46  
47  
48  
49  
50  
51  
52  
53  
54  
55  
56  
57  
58  
59  
60  
61  
62  
63  
64  
65
- [8] Marksberry PK, Jawahir IS (2008) A comprehensive tool-wear/tool-life performance model in the evaluation of NDM (near dry machining) for sustainable manufacturing. *Int J Mach Tools Manuf* 48:878–886.
  - [9] Ulatan D, Ozel T (2011) Machining induced surface integrity in titanium and nickel alloys: A review. *Int J Mach Tools Manuf* 51:250–280.
  - [10] Ezugwu EO (2005) Key improvements in the machining of difficult-to-cut aerospace superalloys. *Int J Mach Tools Manuf* 45:1353–1367.
  - [11] Hong SY, Zhao Z (1999) Thermal aspects, material considerations and cooling strategies in cryogenic machining. *Clean Prod Proc* 1(2):107-116.
  - [12] Hong SY, Ding Y (2001) Micro-temperature manipulation in cryogenic machining of low carbon steel. *J Mater Proc Technol* 116(1):22-30.
  - [13] Hong SY, Broome M (2000) Economical and ecological cryogenic machining of AISI 304 austenitic stainless steel. *Clean Prod Proc* 2(3):157–166.
  - [14] Hong SY, Ding Y, Ekkens RG (1999) Improving low carbon steel chip breakability by cryogenic chip cooling. *Int J Mach Tools Manuf* 39:1065-1085.
  - [15] O’Sullivan D, Cotterell M (2001) Temperature measurement in single point turning. *J Mater Proc Technol* 118:301–308.
  - [16] Hong SY, Ding Y (2001) Cooling approaches and cutting temperatures in cryogenic machining of Ti-6Al-4V. *Int J Mach Tools Manuf* 41:417-1437.
  - [17] Hong SY, Ding Y, Jeong J (2002) Experimental evaluation of friction and liquid nitrogen lubrication effect in cryogenic machining. *Mach Sci Technol* 6(2):235-250.
  - [18] Yildiz Y, Nalbant M (2008) A review of cryogenic cooling in machining processes. *Int J Mach Tools Manuf* 48:947-964.
  - [19] Ezugwu EO, Bonney J, Da Silva RB, Cakir O (2007) Surface integrity of finished turned Ti–6Al–4V alloy with PCD tools. *Int J Mach Tools Manuf* 47:884–891.

- 1  
2  
3  
4  
5  
6  
7  
8  
9  
10  
11  
12  
13  
14  
15  
16  
17  
18  
19  
20  
21  
22  
23  
24  
25  
26  
27  
28  
29  
30  
31  
32  
33  
34  
35  
36  
37  
38  
39  
40  
41  
42  
43  
44  
45  
46  
47  
48  
49  
50  
51  
52  
53  
54  
55  
56  
57  
58  
59  
60  
61  
62  
63  
64  
65
- [20] Zurecki Z, Ghosh R, Frey JH (2003) Investigation of white layer formed in conventional and cryogenic hard turning of steels, in: Proc. ASME Int. Mechanical Engineering Congress and Exposition (IMECE 2003), Washington, DC, USA, November 2003, ASME Pub., pp. 16–21.
- [21] Pusavec F, Hamdi H, Kopac J, Jawahir IS (2011) Surface integrity in cryogenic machining of nickel based alloy-inconel 718. *J Mater Proc Technol* 211(4): 773-783.
- [22] Pu Z, Outeiro JC, Batista AC, Dillon Jr. OW, Puleo DA, Jawahir IS (2012) Enhanced surface integrity of AZ31B Mg alloy by cryogenic machining towards improved functional performance of machined components, *Int J Mach Tools Manuf* 56:17-27.
- [23] Jawahir IS, Pu Z, Yang S, Rotella G, Kaynak Y, Lu T, Deshpande A, Umbrello D, Dillon Jr. OW (2012) Cryogenic Processing of Materials for Enhanced Product Life, Performance and Sustainability, in: 15th Int. Conf. on Advances in Materials & Processing Technologies (AMPT 2012) Keynote paper, in press.
- [24] Dhar NR, Paul S, Chattopadhyay AB (2002) Machining of AISI 4140 steel under cryogenic cooling—tool wear, surface roughness and dimensional deviation, *J Mater Proc Technol* 123/3:483-489.
- [25] Umbrello D, Micari F, Jawahir IS (2012) The effects of cryogenic cooling on surface integrity in hard machining: A comparison with dry machining. *CIRP Annals – Manuf Technol* 61(1):103-106.
- [26] Wang ZY, KP Rajurkar (2000) Cryogenic machining of hard-to-cut materials, *Wear* 239:168–175.
- [27] Dhananchezian M, Pradeep Kumar M (2011) Cryogenic turning of the Ti–6Al–4V alloy with modified cutting tool inserts. *Cryogenics* 51:34–40.
- [28] Sadeghi MH, Haddad MJ, Tawakoli T, Emami M (2009) Minimal quantity lubrication-MQL in grinding of Ti–6Al–4V titanium alloy. *Int J Adv Manuf Technol* 44:487–500.

- 1  
2  
3  
4  
5  
6  
7  
8  
9  
10  
11  
12  
13  
14  
15  
16  
17  
18  
19  
20  
21  
22  
23  
24  
25  
26  
27  
28  
29  
30  
31  
32  
33  
34  
35  
36  
37  
38  
39  
40  
41  
42  
43  
44  
45  
46  
47  
48  
49  
50  
51  
52  
53  
54  
55  
56  
57  
58  
59  
60  
61  
62  
63  
64  
65
- [29] McClung RC (2007) A literature survey on the stability and significance of residual stresses during fatigue, *Fatigue Fract Eng Mater Struct* 30:73–205.
- [30] Donachie Jr. MJ (2000) *Titanium: A Technical Guide*, ASM International, Materials Park, OH 44073–000.
- [31] Chan KS (2003) A Microstructure-Based Fatigue-Crack-Initiation Model. *Metall Mater Trans* 34/A:43–58.
- [32] Chan KS (2009) Changes in fatigue life mechanism due to soft grains and hard particles. *Int J Fatigue* 32:526–534.
- [33] Chan KS (2010) Roles of microstructure in fatigue crack initiation. *Int J Fatigue* 32:1428–1447.
- [34] Rotella G, Lu T, Settineri L, Dillon Jr. OW, Jawahir IS (2012) Dry and Cryogenic Machining: Comparison from the Sustainability Perspective, in: G. Seliger (Ed.) *Sustainable Manufacturing*, Springer-Verlag Berlin Heidelberg, pp. 95–100.
- [35] JCPDS – International Centre for Diffraction Data, Powder Diffraction File, Inorganic Phases, Sets 1-60, 2010.
- [36] Zeng L, Bieler TR (2005) Effects of working, heat treatment, and aging on microstructural evolution and crystallographic texture of  $\alpha$ ,  $\alpha'$ ,  $\alpha''$  and  $\beta$  phases in Ti–6Al–4V wire. *Mater Sci Eng A* 392:403–414.
- [37] Herbert C, Axinte D, Hardy M, Brown PD (2012) Investigation into the characteristics on the white layers produced in a nickel-based superalloy from drilling operations. *Mach Sci Technol* 16(1):40-52.
- [38] Fan Y, Cheng P, Yao YL (2005) Effect of phase transformations on laser forming of Ti–6Al–4V alloy. *J Applied Phys* 98:013518 – 013518-9.
- [39] Pederson R, Babushkin O, Skystedt F, Warren R (2003) Use of high temperature X-ray diffractometry to study phase transitions and thermal expansion properties in Ti-6Al-4V. *Mater Sci Technol* 19(11):1533–1538.



1  
2  
3  
4  
5  
6  
7  
8  
9  
10  
11  
12  
13  
14  
15  
16  
17  
18  
19  
20  
21  
22  
23  
24  
25  
26  
27  
28  
29  
30  
31  
32  
33  
34  
35  
36  
37  
38  
39  
40  
41  
42  
43  
44  
45  
46  
47  
48  
49  
50  
51  
52  
53  
54  
55  
56  
57  
58  
59  
60  
61  
62  
63  
64  
65

## FIGURES

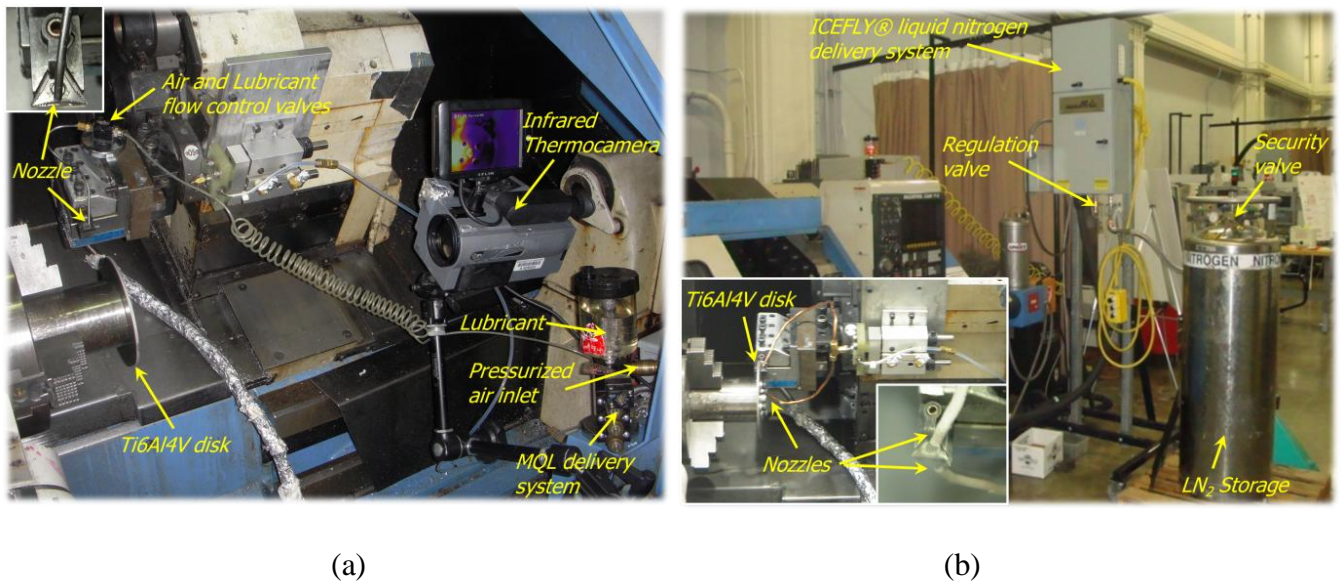
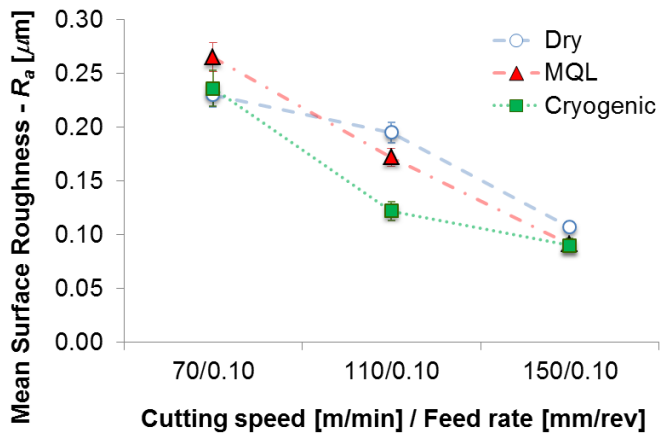
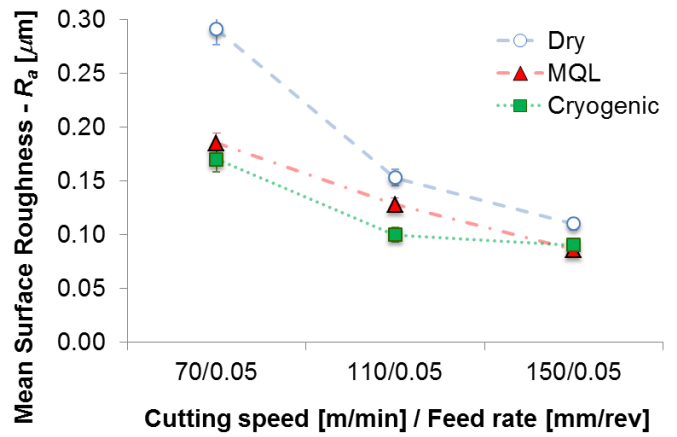


**Figure 1.** Experimental set-up for orthogonal cutting tests with (a) MQL and (b) cryogenic cooling systems.



(a)



(b)

**Figure 2.** Mean surface roughness on machined samples under dry, MQL and cryogenic cooling conditions.

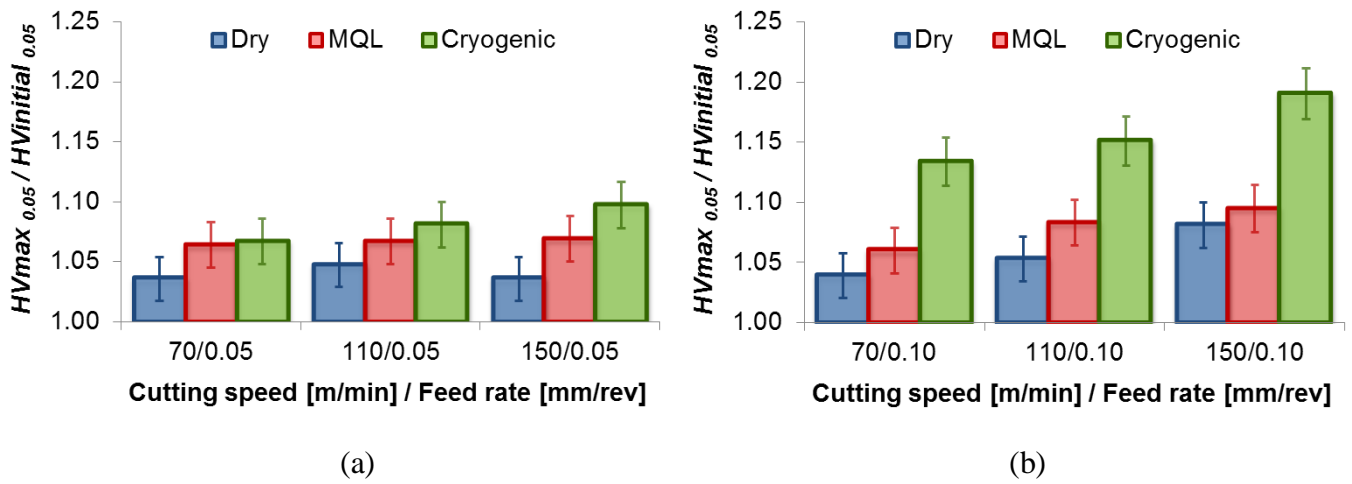


**Figure 3.** The measured surface hardness at varying cutting speeds for (a) 0.05 mm/rev and (b) 0.10 mm/rev feedrate.

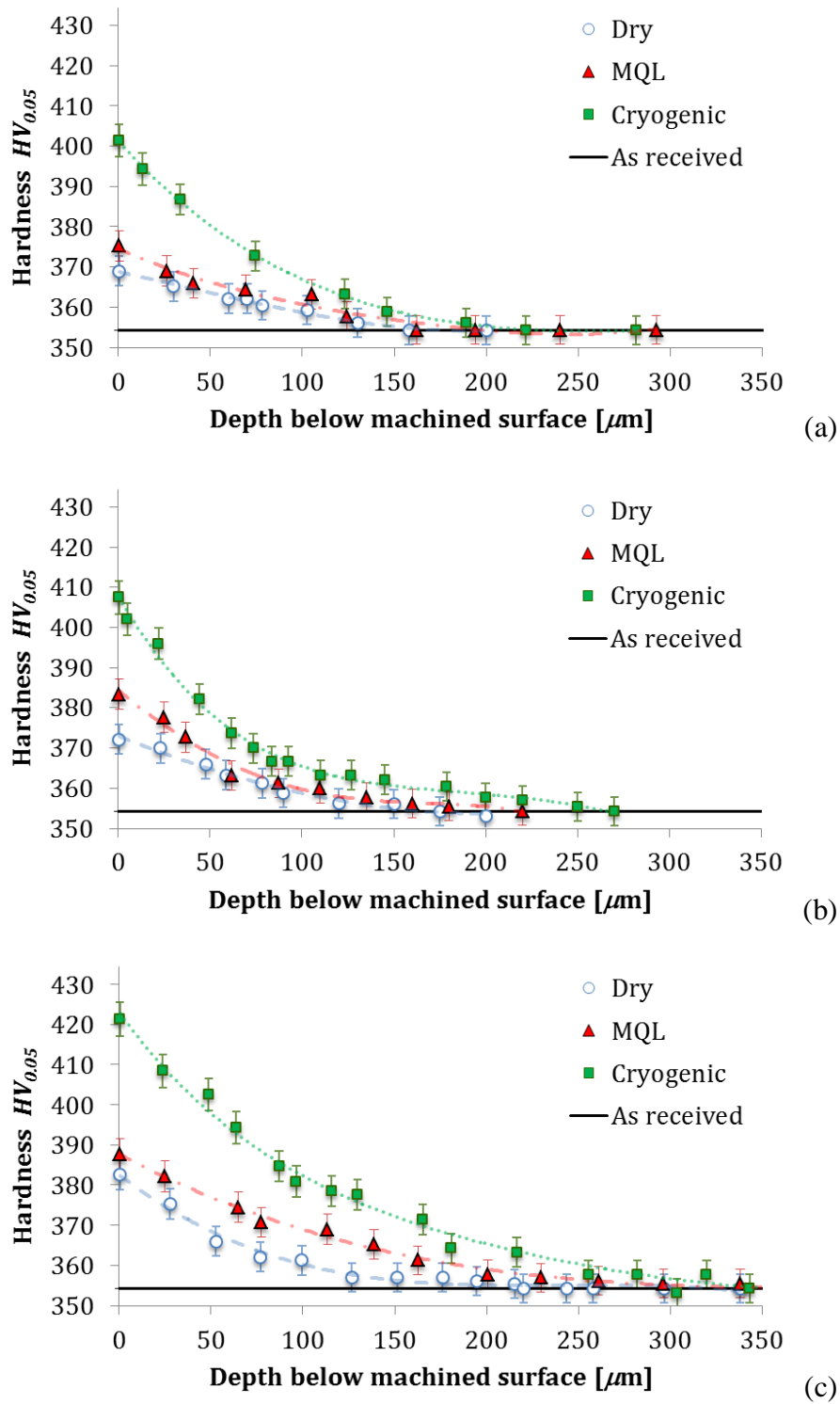


**Figure 4.** Surface and sub-surface hardness profiles for experimental conditions at  $f = 0.1 \text{ mm/rev}$  and cutting speed of (a)  $70 \text{ m/min}$ , (b)  $110 \text{ m/min}$  and (c)  $150 \text{ m/min}$ .

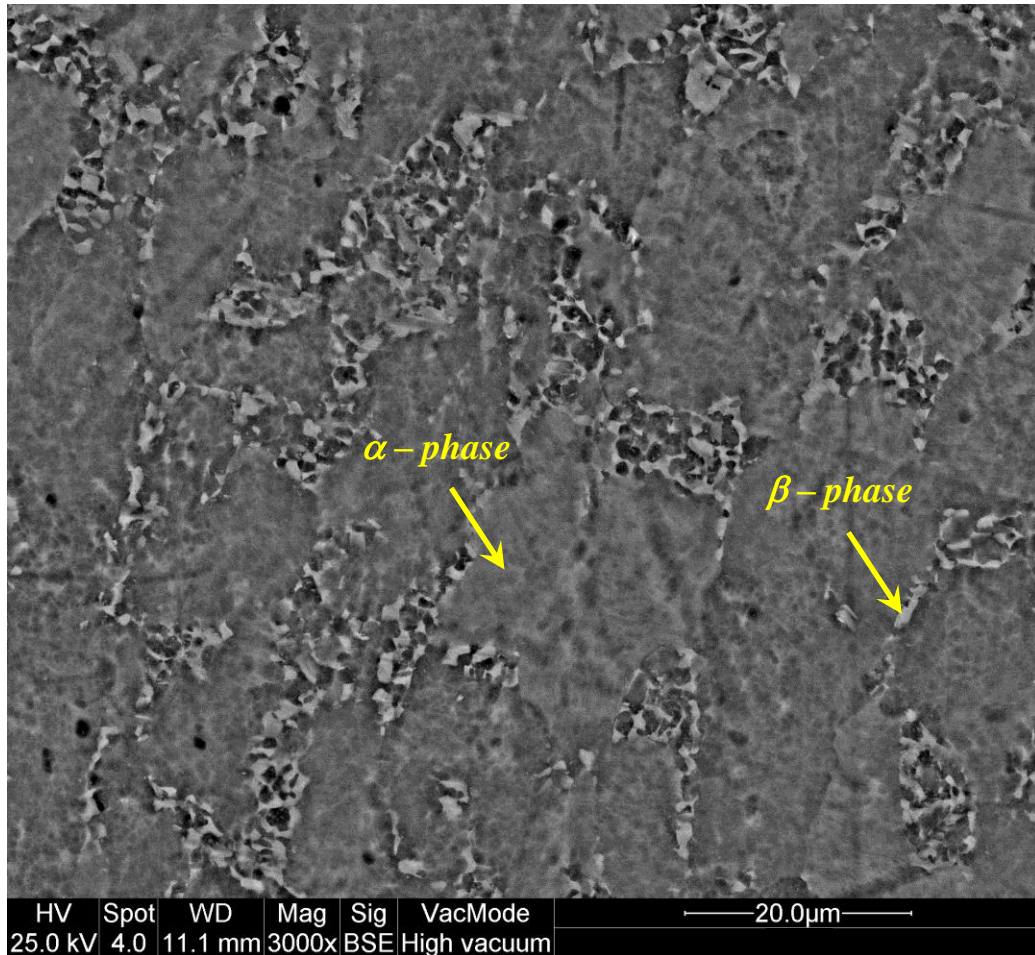


**Figure 5.** SEM micrograph of an etched microstructure of the as-received *Ti6Al4V* with dark region for HCP  $\alpha$  phase and light region for BCC  $\beta$  phase.

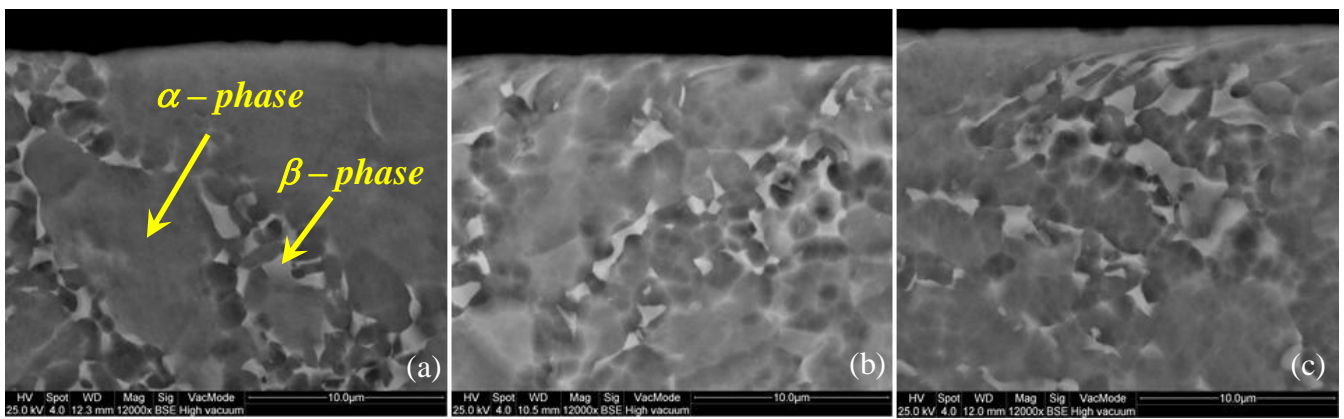


**Figure 6.** SEM images of the machined samples under (b) dry, (c) MQL, and (d) cryogenic conditions at  $v_c = 150$  m/min, and  $f = 0.05$  mm/rev. ( $\alpha$  – dark grains;  $\beta$  – light grains).

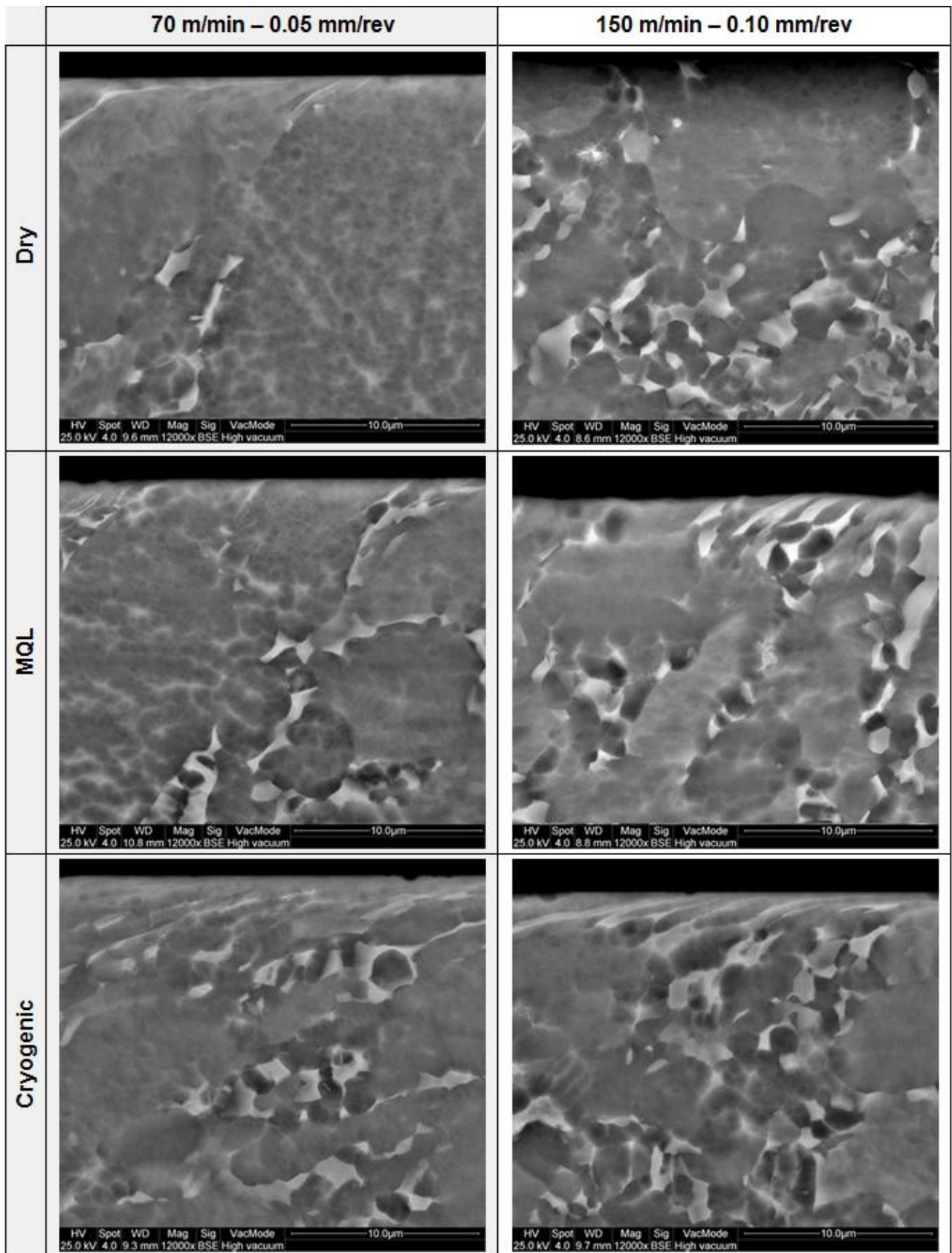
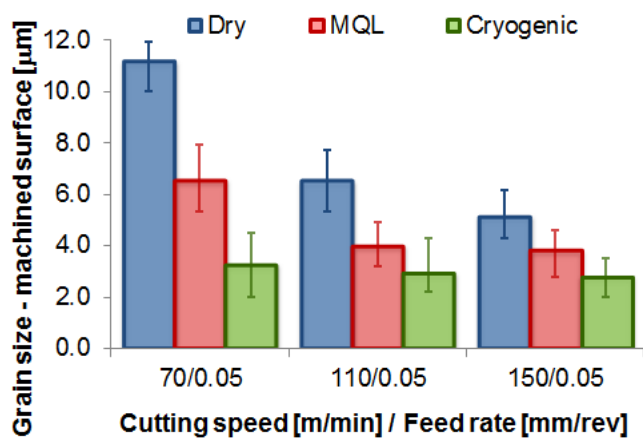
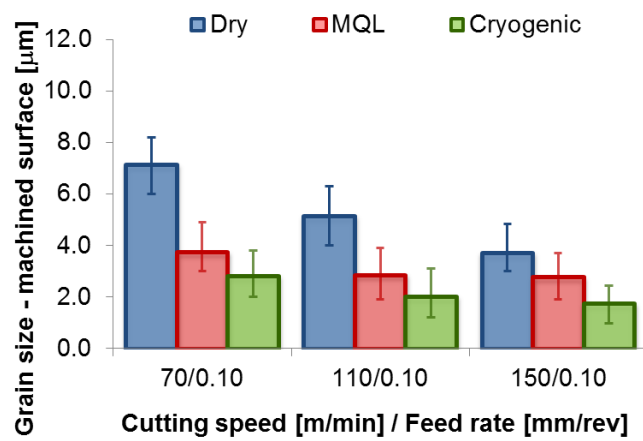


**Figure 7.** SEM images of the machined samples under dry, MQL, and cryogenic conditions at different cutting speeds and feed rates ( $\alpha$  – dark grains;  $\beta$  – light grains).





(a)



(b)

**Figure 8.** Comparison of measured grain size variation at varying the cutting speed: (a) 0.05 mm/rev; (b) 0.10 mm/rev.

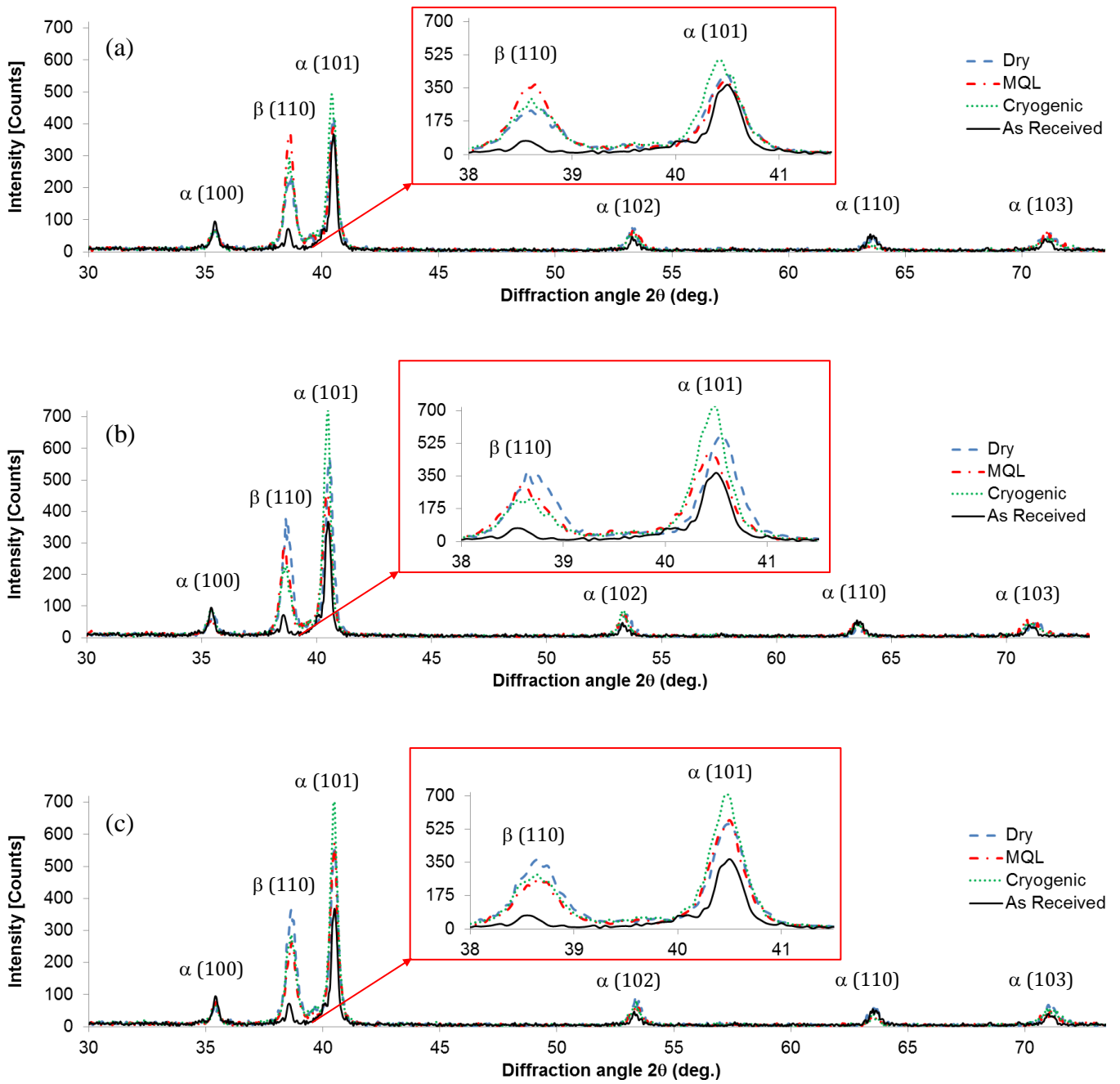


**Figure 9.** XRD results obtained for machined samples at (a)  $v_c = 70$  m/min, and  $f = 0.05$  mm/rev; (b)  $v_c = 150$  m/min, and  $f = 0.05$  mm/rev; (c)  $v_c = 150$  m/min, and  $f = 0.10$  mm/rev.

***TABLES*****Table 1**

Experimental test conditions.

$v_c$ [m/min]	70	110	150	70	110	150
$f$ [mm/rev]	0.05			0.10		
Cooling	Dry, Cryogenic, MQL			Dry, Cryogenic, MQL		